IRAQI JOURNAL OF APPLIED PHYSICS
Vol. 22, No. 2, April-June 2026, pp. 299-304

Effect of Nitrogen Gas Flow Rate on Synthesis of Highly-Pure Titanium Nitride Nanopowders via Carbothermal Reduction and Nitridation

Hayder G. Fahad
Oday A. Hammadi*
Rand B. Lutfi
Sohaib S. Ahmed

Department of Physics,
College of Education,
Al-Iraqia University,
Baghdad, IRAQ
Corresponding author email:
oday.hammadi@aliraqia.edu.iq

In this work, titanium nitride nanopowders were prepared by the carbothermal reduction method. A mixture of titanium dioxide nanopowder and carbon black at molar ratio of 2.2:1 was milled using high energy ball milling (HEBM), heated up to 1300°C inside tube furnace with nitrogen gas flowing at different rates (100, 300, or 500 sccm). The structural characteristics show that the prepared nanopowders are polycrystalline with minimum particle size of 25-30 nm. These nanopowders showed high structural purity as no traces for elements other than titanium and nitrogen were detected with small inevitable amount of carbon. The absorption spectra of the prepared nanopowders were apparently sensitive to the flow rate of nitrogen gas inside vacuum chamber while the structural characteristics was less sensitive. This work can be very successful to produce highly-pure titanium nitride nanopowders at low production cost, high reliability and low complexity.

Keyword: Titanium nitride; Nanopowders; Carbothermal reduction; Nitridation
Received: 25 September 2025; Revised: 7 January 2026; Accepted: 14 January 2026; Published: 1 April 2026

1. Introduction

Titanium nitride (TiN) stands as an exceptionally durable ceramic compound prized for its outstanding mechanical hardness, resistance to extreme temperatures, and electrical conductivity comparable to metals [1,2]. These characteristics have established its widespread use in protective coatings, precision machining tools, and advanced electronic components [3]. The material crystallizes in a face-centered cubic arrangement similar to table salt, displaying a distinctive golden hue while boasting extraordinary thermal resilience with a melting point approaching 3000°C [4,5]. Its chemical stability remains impressive, withstanding oxidative environments up to 800°C and demonstrating tolerance to both acidic and alkaline conditions - properties derived from the strong covalent bonding between titanium and nitrogen atoms [6]. When engineered at the nanoscale, TiN manifests as nanoparticles, nanorods, or ultrathin films that exhibit novel phenomena including enhanced catalytic performance, unique light-matter interactions, and optical properties that can be precisely adjusted by controlling particle dimensions and architecture [7-9].

Modern fabrication approaches for TiN nanomaterials encompass both physical and chemical synthesis routes. Conventional methods like magnetron sputtering and chemical vapor deposition (CVD) typically require elevated temperatures between 800-1000°C where titanium compounds react with nitrogen sources [10-12]. More innovative techniques such as plasma-assisted CVD (PACVD) or solution-based sol-gel methods allow for processing at substantially reduced temperatures [13-15]. Alternative production strategies include high-energy ball milling and pulsed laser ablation, which are particularly effective for generating ultrafine nanoparticles [16,17].

The thermal synthesis of titanium nitride relies on the carbothermal reduction and nitridation (CRN) of titanium dioxide (TiO_2) in presence of carbon source and nitrogen environment [18,19]. The overall reaction is endothermic and can be described by the following:

$$TiO_2(s) + 2C(s) + \frac{1}{2}N_2(g) \rightarrow TiN(s) + 2CO(g)$$

From a thermodynamic viewpoint, the standard Gibbs free energy change ($\Delta G°$) for this reaction becomes negative only at elevated temperatures (>1500K) at atmospheric pressure. The reaction is driven by the increase in entropy due to the evolution of carbon monoxide gas [20].

The transformation from oxide to nitride is not a single-step process, instead, the reduction mechanism is mostly described by the constructive conversion model [21,22]. The reduction sequence can be explained as follows:

TiO_2 (Anatase/Rutile) → Ti_nO_{2n-1} (Magnéli phases) → Ti_3O_5 → Ti_2O_3

As the oxygen is removed, both carbon and nitrogen diffuse into the lattice, often forming a solid solution intermediate, titanium oxycarbonitride ($TiC_xN_yO_z$) before finally stabilizing as a cubic TiN [23].

To produce nanopowder rather than bulk micro-powder, the nucleation and growth should be precisely addressed. The carbothermal reduction is a diffusion-controlled reaction as the solid-solid diffusion between carbon and titanium dioxide is the rate-limiting step. As well, in HEBM, high densities of dislocations and defects are mostly resulted. These defects lower the activation energy required for the reaction, allowing

 © ALL RIGHTS RESERVED

synthesis at lower temperatures (1100-1200°C) and inhabiting excessive grain growth [24-26]. Post-synthesis thermal treatment is frequently employed to perfect the crystalline quality, though special precautions must be implemented to avoid atmospheric contamination during material handling [27-30].

The practical implementations of TiN span an impressive range of technologies. In industry, it dramatically improves the durability of precision cutting implements and forming dies through its exceptional wear resistance [31-33]. The microelectronics industry utilizes it extensively as conductive interconnects and protective barriers in integrated circuits due to its excellent electrical properties and compatibility with silicon processing [34,35]. Energy storage systems incorporate TiN nanostructures to boost the performance of supercapacitor components, taking advantage of their combined electrical conductivity and electrochemical durability [36,37]. Medical applications benefit from its biocompatible nature and microbial resistance in prosthetic devices and surgical tools [38,39]. Its unique interaction with light enables applications in advanced optical sensors and targeted cancer therapies [40]. Cutting-edge research continues to explore novel uses in environmental remediation through photocatalytic processes and clean energy generation via water splitting, capitalizing on its ability to harness visible light while maintaining structural integrity [41-44].

While TiN presents numerous advantages, manufacturing challenges remain in producing nanomaterials with consistent particle characteristics at industrial scales cost-effectively [45,46]. Current research works focus on developing composite systems combining TiN with carbon nanomaterials to create synergistic materials for next-generation applications [47-49]. The exceptional combination of mechanical strength, chemical stability, and functional versatility ensures titanium nitride's continued importance across both established industrial sectors and emerging high-tech fields, with ongoing research continually uncovering new potential applications for this remarkable material [50-53].

In this work, titanium nitride nanopowders were prepared by the carbothermal reduction and nitridation method of the solid mixture of carbon black and titanium dioxide inside tube furnace in presence of flowing nitrogen gas. The structural and spectroscopic characteristics of the prepared nanopowders are studied to introduce the effect of nitrogen gas flow rate on these characteristics.

2. Experimental Part

The raw materials used in this work included titanium dioxide (TiO_2), carbon black and nitrogen (N_2) gas. Anatase TiO_2 nanopowder of 99.9% purity and average particle size of <20nm was extracted from thin film sample deposited on glass substrates by dc reactive magnetron sputtering technique. Figure (1) shows the FE-SEM image of the anatase TiO_2 nanopowder sample used in this work. The anatase phase was selected due to its lower surface energy and higher reactivity [54,55]. More details on the preparation of this material can be found elsewhere [56-63]. Carbon black powder was supplied by Nanografi Advanced Materials with 99.99% purity, 4 μm particle size, 1.79 g/cm^3 density and high specific surface area (>70 m^2/g). The carbon black was mixed with TiO_2 nanopowder at a molar ratio of C:TiO_2 = 2.2:1. A slight excess of ≤10% of carbon is often used to balance the oxidation losses and ensure complete removal of oxygen.

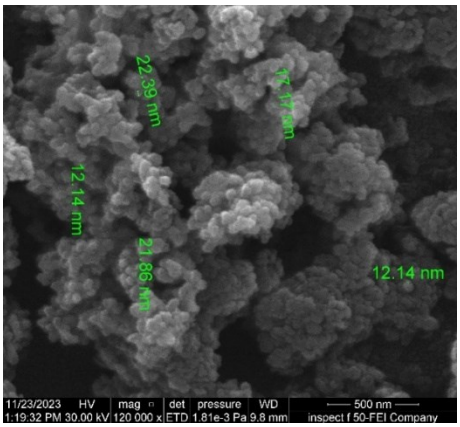

Fig. (1) The FE-SEM image of the anatase TiO_2 nanopowder sample used in this work

The mixture was milled using a Torontech BM20 planetary ball mill with tungsten carbide (WC) as ball material to minimize contamination. The ball-to-powder ratio was 20:1, milling speed was 450 rpm for 6 hours with ethanol a control agent for wetting to prevent the agglomeration during milling. The carbothermal reduction was carried out in a horizontal tube furnace as a reactor with alumina tube through which highly-pure nitrogen gas flows at flow rates of 100, 300, or 500 sccm. It is essential to sweep away the produced carbon monoxide (CO) gas and hence shifting the equilibrium to the right according to Le Chatelier's principle. The effect of nitrogen gas flow rate on the characteristics of the produced materials was introduced. The carbothermal reduction contains three consecutive stages depending on temperature range and duration. First, ramp up stage is started from room temperature (R.T.) up to 1100°C with ramp rate of 10°C/min. second, the isothermal reaction continues at temperature range of 1100-1300°C for 3 hours. Third, the natural cooling from 1300°C down to room temperature during ~3 hours.

A post-processing or decarburization step was performed to remove the residual carbon from the sample, which appeared dark grey. This step includes calcination at 450°C in air for one hour to burn off the

 © ALL RIGHTS RESERVED

residual free carbon without oxidizing the TiN back to TiO_2.

The structural, morphological and spectroscopic characteristics of the prepared sample were determined by x-ray diffraction (XRD) using PanAnalytical ARIES x-ray diffractometer, field-emission scanning electron microscopy (FE-SEM) using FEI Inspect^{TM} 50 FE-SEM instrument, energy-dispersive x-ray spectroscopy (EDX), and UV-visible spectrophotometry using SpectraAcademy KMAC SV2100 UV-visible spectrophotometer.

3. Results and Discussion

Figure (2) shows the XRD patterns of the titanium nitride nanopowder samples prepared in this work at different flow rates of nitrogen gas through the tube furnace (100, 300, and 500 sccm). A polycrystalline NaCl-like structure is recognized in all samples with five distinct sharp diffraction peaks at 2θ of 36.82°, 42.79°, 62.07°, 74.42°, and 78.33° those corresponding to the crystal planes of (111), (200), (220), (311), and (222), respectively. This result was confirmed by the JCPDS card no. 87-0633.

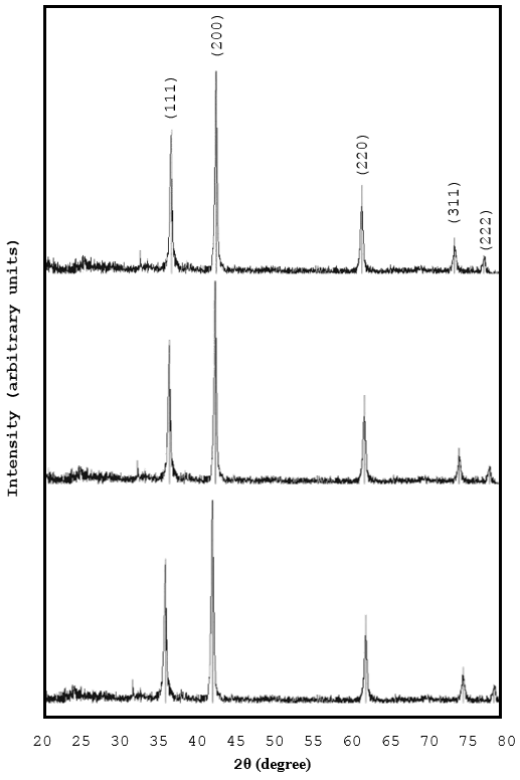

Fig. (2) XRD patterns of TiN nanopowders prepared in this work (upper: 100 sccm, middle: 300 sccm, lower: 500 sccm)

The average crystallite size of TiN was estimated for the sample prepared at nitrogen gas flow rate of 500 sccm, using Scherrer's equation from the full width at half maximum (FWHM) of the most intense peak (200) and was found to be 18 nm. All the prepared samples exhibited a highly similar crystalline structure, which can be attributed to the effectiveness of the tube furnace in purging the reaction environment of contaminants and air components such as carbon dioxide and water vapor. These elements have adverse effects on the formation of nanomaterials through chemical reactions. A difference in the crystallinity of the synthesized material was observed with variations in the nitrogen gas pumped into the reaction chamber as one of the reactants. The crystallinity increased with higher nitrogen gas flow rate due to the greater total volume of reacting species. This is particularly significant given that TiO_2 is a solid material capable of providing a very large number of particles that can react with nitrogen ions generated by thermal activation.

Figure (3) shows the absorption spectra of the of titanium nitride nanopowders prepared in this work at three different nitrogen gas flow rates of 100, 300, and 500 sccm within the spectral range of 300-750 nm. The samples prepared at nitrogen gas flow rates of 100 and 300 sccm show high absorption in the UV region that decreases sharply to reach its minimum at 375 nm, while the sample prepared at nitrogen gas flow rate of 500 sccm shows similar behavior but the minimum value was slightly shifted to 370 nm. This behavior corresponds to energy band gap of 3.31-3.35 eV, which is approximately within the typical range of energy band gap of titanium nitride (3.35-3.45 eV) [39-41]. The slight shift in the absorption edge may be originated from the obvious semi-metallic behavior of titanium nitride that would originate a surface plasmon resonance during the absorption of UV-visible radiation [42].

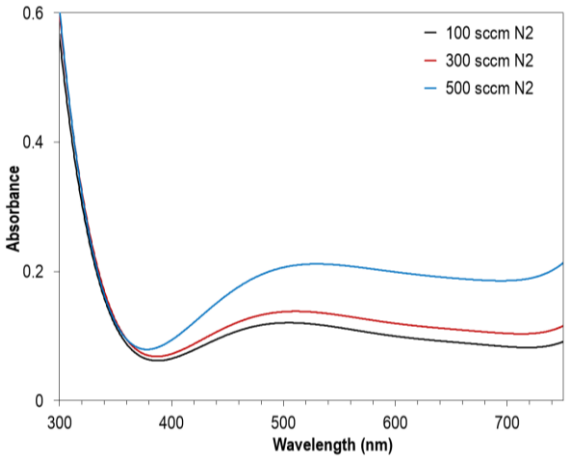

Fig. (3) Absorption spectra of the titanium nitride nanopowders prepared in this work at three different nitrogen gas flow rates (100, 300, and 500 sccm)

A slight increase in the absorbance is seen and a broad peak can be observed at 505 nm before slightly decreases and keeps an approximately constant value at wavelengths longer than 600 nm. The increase in absorbance with increasing nitrogen gas flow rate used for the preparation of the material agrees to the

 © ALL RIGHTS RESERVED

principle of Beer-Lambert law as the concentration of the medium is increased with the formation of more titanium nitride molecules due to the increase in nitrogen gas content.

Based on the observed similarity in the crystalline structure and spectroscopic behavior of the prepared samples, only the sample prepared at nitrogen gas flow rate of 500 sccm was examined using field-emission scanning electron microscopy (FE-SEM) to analyze its surface morphology and condition. The FE-SEM image in Fig. (4) reveals that the nanomaterial surface was highly homogeneous, with particles exhibiting a largely uniform shape and no significant agglomeration or particle clustering. The minimum particle size is ranging within 25-30 nm. These favorable characteristics can be attributed to the nature of thermal reduction process carried out inside tube furnace as an energetically uniform and highly homogeneous environment, ensuring even distribution of the energy required for nanoparticle formation and growth among the reactant species. Additionally, it significantly reduces energy losses compared to conventional methods.

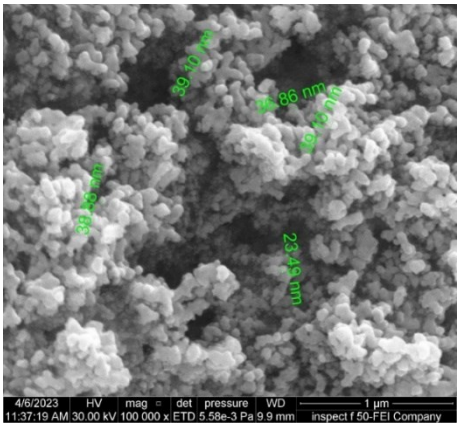

Fig. (4) The FE-SEM image of the titanium nitride nanopowder prepared in this work at nitrogen gas flow rate of 500 sccm

Figures (5) and (6) show the EDX spectrum and spatial distribution of the elements (N, Ti, and C) found in the prepared nanopowder sample prepared at nitrogen gas flow rate of 500 sccm. The atomic content of the sample shows that the prepared compound is very close to the stoichiometry, which can be an additional advantage for the preparation method. The trace of carbon in the sample is inevitable due to the use of carbon black as well the mounting method inside EDX equipment. In Fig. (6), the nitrogen signal is widespread across the field of view but appears less intense and slightly non-uniform in some regions, especially the bottom-left corner which is significantly darker. This could suggest either a lower nitrogen content or possible shadowing effect in that region. Some agglomeration or thickness variation may affects x-ray detection. Titanium is uniformly distributed throughout the sample area with high signal intensity, which indicates a homogeneous presence of titanium, as expected in a TiN compound. The sources of carbon appeared in the final sample are the carbon black and the experimental setup of the EDX instrument.

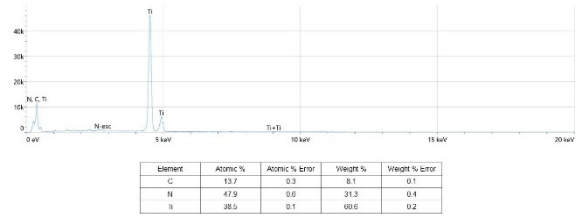

Element	Atomic %	Atomic % Error	Weight %	Weight % Error
C	13.7	0.3	8.1	0.1
N	47.9	0.6	31.3	0.4
Ti	38.5	0.1	60.6	0.2

Fig. (5) EDX spectrum of the titanium nitride nanopowder prepared in this work at nitrogen gas flow rate of 500 sccm

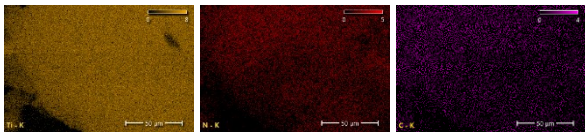

Fig. (6) Color mapping analysis of the elements N, Ti, and C found in of the titanium nitride nanopowder prepared in this work at nitrogen gas flow rate of 500 sccm

4. Conclusion

The carbothermal reduction of solid solution of titanium dioxide and carbon black in presence of flowing nitrogen gas was efficiently performed to produce highly-pure titanium nitride nanopowders. This reaction requires was carried out at high temperature (up to 1300°C) inside a horizontal tube furnace. It was found that the higher flow rate of nitrogen gas can enhance the structural and optical characteristics of the produced titanium nitride nanomaterial. The nanomaterial prepared by this technique can be used for various spectroscopic, environmental, and biomedical applications that requires highly-pure nanomaterials.

References

[1] A.N. Ermakov et al., "Formation of complex titanium-nickel nitride $Ti_{0.7}Ni_{0.3}N$ in the "core-shell" structure of TiN-Ni", *Int. J. Refract. Metals Hard Mater.*, 84 (2019) 104996.

[2] A.S. Abiyev, E.M. Huseynov and R.F. Hashimov, "Gamma radiation-induced alterations in nanocrystalline titanium nitride (TiN) particles: A structural perspective", *Radiat. Phys. Chem.*, 218 (2024) 111638.

[3] A. Chu et al., "Preparation of TiN nanopowder by carbothermal reduction of a combustion synthesized precursor", *Mater. Characteriz.*, 81 (2013) 76-84.

[4] A. Rajabi et al., "Novel precursor of nitrogen for the synthesis of $TiC_{0.7}N_{0.3}$ through vacuum oven-induced combustion", *Ceram. Int.*, 46(7) (2020) 9271-9280.

[5] A. Ghazal et al., "Plasmonic titanium nitride-based membranes for solar-driven domestic wastewater distillation treatment", *Chem. Eng. J.*, 484 (2024) 149594.

 © ALL RIGHTS RESERVED

[6] B. Bora et al., "Studies on a supersonic thermal plasma expansion process for synthesis of titanium nitride nanoparticles", *Powder Technol.*, 246 (2013) 413-418.

[7] B.M. Moshtaghioun et al., "Titanium carbonitride fabricated by spark plasma sintering: Is it a ceramic model of carbon-induced Friedel-Fleisher strengthening effect?", *J. Euro. Ceram. Soc.*, 41(13) (2021) 6275-6280.

[8] B.H. Liu et al., "Linking microstructure evolution and impedance behaviors in spark plasma sintered Si_3N_4/TiC and Si_3N_4/TiN ceramic nanocomposites", *Ceram. Int.*, 39(4) (2013) 4205-4212.

[9] B.M. Moshtaghioun, D. Gómez-García and A. Domínguez-Rodríguez, "Spark plasma sintering of titanium nitride in nitrogen: Does it affect the sinterability and the mechanical properties?", *J. Euro. Ceram. Soc.*, 38(4) (2018) 1190-1196.

[10] C. Mendoza et al., "Improvement of TiN nanoparticles EPD inducing steric stabilization in non-aqueous suspensions", *J. Euro. Ceram. Soc.*, 36(2) (2016) 307-317.

[11] C.U. Bang, Y.C. Hong and H.S. Uhm, "Synthesis and characterization of nano-sized nitride particles by using an atmospheric microwave plasma technique", *Surf. Coat. Technol.*, 201(9–11) (2007) 5007-5011.

[12] O.A. Hamadi, "The Fundamentals of Plasma-Assisted CVD Technique Employed in Thin Films Production", *Iraqi J. Appl. Phys. Lett.*, L1(2) (2008) 3-8.

[13] D.V. Mashtalyar et al., "Plasma electrolytic oxidation of the magnesium alloy MA8 in electrolytes containing TiN nanoparticles", *J. Mater. Sci. Technol.*, 33(5) (2017) 461-468.

[14] D.V. Mashtalyar et al., "Hard wearproof PEO-coatings formed on Mg alloy using TiN nanoparticles", *Appl. Surf. Sci.*, 503 (2020) 144062.

[15] P. Mouchani, R. Sarraf-Mamoory and H. Aghajani, "Preparation of titanium nitride/oxynitride nanotube array via ammonia-free PECVD method for enhancing supercapacitor performance", *J. Alloys Comp.*, 904 (2022) 163895.

[16] E. Yousefi et al., "Preparation of new titanium nitride-carbon nanocomposites in supercritical benzene and their oxygen reduction activity in alkaline medium", *Electrochimica Acta*, 164 (2015) 114-124.

[17] O.E. Falodun et al., "Fabrication and Microstructural Characterization of Nanoparticle TiN Reinforced Al-Mg-Si Matrix Composite", *Materials Today: Proc.*, 18(7) (2019) 3209-3217.

[18] V.C. Deivayanai et al., "Fused deposition modeling of functional nanohybrids: a transformative approach to sustainable water purification", *Result. Eng.*, 28 (2025) 108289.

[19] S. Kumar et al., "Developments, challenges, and projections in solar battery charging in India", *Result Eng.*, 24 (2024) 103248.

[20] A. Bin Yousaf et al., "Strategies to mitigate the challenges in methanol oxidation reaction with contemporary platinum-based electrocatalysts", *J. Power Sour.*, 653 (2025) 237686.

[21] R.B. Rajput et al., "Recent developments in ZnO-based heterostructures as photoelectrocatalysts for wastewater treatment: A review", *Enviro. Adv.*, 9 (2022) 100264.

[22] V. Vallejo-Otero et al., "Advancements in nitridation of TiO_2 layers: Mechanisms, techniques, and applications for TiN thin films", *J. Euro. Ceram. Soc.*, 45(10) (2025) 117330.

[23] B. Wang, S. Shen and S.S. Mao, "Black TiO_2 for solar hydrogen conversion", *J. Materiomics*, 3(2) (2017) 96-111.

[24] N. Madima et al., "Recent advances in the development of defective black TiO_2 nanomaterials for application in energy and environmental sustainability: A review", *Result. Eng.*, 26 (2025) 104868.

[25] A. Islam et al., "Progress in silicon-based materials for emerging solar-powered green hydrogen (H_2) production", *Adv. Colloid Interface Sci.*, 343 (2025) 103558.

[26] Y. Sani et al., "Enhanced electromagnetic microwave absorbing performance of carbon nanostructures for RAMs: A review", *Appl. Surf. Sci. Adv.*, 18 (2023) 100455.

[27] O.E. Falodun et al., "Effect of sintering parameters on densification and microstructural evolution of nano-sized titanium nitride reinforced titanium alloys", *J. Alloys Comp.*, 736 (2018) 202-210.

[28] G.N. Mekgwe et al., "Fabrication of graphite reinforced TiC_xN_y by spark plasma sintering technique: A comparative assessment of microstructural integrity and nanoindentation properties", *Vacuum*, 187 (2021) 110144.

[29] P. Simon et al., "X-ray absorption investigation of titanium oxynitride nanoparticles obtained from laser pyrolysis", *Chem. Phys.*, 418 (2013) 47-56.

[30] R. Aghababazadeh et al., "Synthesis and characterization of nanocrystalline titanium nitride powder from rutile and anatase as precursors", *Surf. Sci.*, 601(13) (2007) 2881-2885.

[31] S. Farooq et al., "Thermo-optical performance of bare laser-synthesized TiN nanofluids for direct absorption solar collector applications", *Sol. Ener. Mater. Sol. Cells*, 252 (2023) 112203.

[32] S.R. Oke et al., "Influence of sintering process parameters on corrosion and wear behaviour of SAF 2205 reinforced with nano-sized TiN", *Mater. Chem. Phys.*, 206 (2018) 166-173.

[33] J. Senthilselvan et al., "Cathodic arc deposition of nanocrystalline titanium nitride thin film on fluorine doped tin oxide coated glass substrate: Crystal structural, microstructural, mechanical, optical and electrical properties", *Ceram. Int.*, 49(23A) (2023) 37072-37088.

[34] S. Suarez-Vazquez and M. Nanko, "Preparation of dense TiN_{1-X} (X=0–0.4) by pulsed electric current sintering: Densification and mechanical behavior", *Int. J. Refract. Metals Hard Mater.*, 44 (2014) 54-59.

[35] S. Ran and L. Gao, "Mechanical properties and microstructure of TiN/TZP nanocomposites", *Mater. Sci. Eng. A*, 447(1–2) (2007) 83-86.

[36] J.-X. Xue et al., "Improved radiation damage tolerance of titanium nitride ceramics by introduction of vacancy defects", *J. Euro. Ceram. Soc.*, 34(3) (2014) 633-639.

[37] X. Hou et al., "Synthesis of titanium nitride nanopowder at low temperature from the combustion synthesized precursor and the thermal stability", *J. Alloys Comp.*, 615 (2014) 838-842.

 © ALL RIGHTS RESERVED

[38] K.-H.T. Dinh et al., "Fabrication of N-doped TiO_2 and TiN nanorods by NH_3 treatment: Evolution of morphology, structures, composition and optical properties", *Ceram. Int.*, 50(7A) (2024) 10241-10251.

[39] L.-Q. Huang and Q. Huang, "High-strength Ti–BN composites with core-shell structured matrix and network-woven structured TiB nanowires", *Trans. Nonferrous Metals Soc. China*, 32(4) (2022) 1169-1177.

[40] Y.C. Hong, D.H. Shin and H.S. Uhm, "Production of vanadium nitride nanopowders from gas-phase $VOCl_3$ by making use of microwave plasma torch", *Mater. Chem. Phys.*, 101(1) (2007) 35-40.

[41] M. Canillas et al., "Bulk Ti nitride prepared from rutile TiO_2 for its application as stimulation electrode in neuroscience", *Mater. Sci. Eng. C*, 96 (2019) 295-301.

[42] M. Drygaś et al., "Aerosol-assisted vapor phase synthesis of powder composites in the target system GaN/TiN for potential electronic applications", *Mater. Res. Bull.*, 40(7) (2005) 1136-1142.

[43] M. Drygas et al., "Structural and magnetic properties of ceramics prepared by high-pressure high-temperature sintering of manganese-doped gallium nitride nanopowders", *J. Euro. Ceram. Soc.*, 36(4) (2016) 1033-1044.

[44] M.Q. Snyder et al., "Synthesis and characterization of atomic layer deposited titanium nitride thin films on lithium titanate spinel powder as a lithium-ion battery anode", *J. Power Sources*, 165(1) (2007) 379-385.

[45] M. Petousis et al., "On the substantial mechanical reinforcement of Polylactic Acid with Titanium Nitride ceramic nanofillers in material extrusion 3D printing", *Ceram. Int.*, 49(10) (2023) 16397-16411.

[46] M.K. Ali and F.J. Kadhim, "Synthesis and Study the Structural and Optical Properties of TiN and TiO_2:TiN Nanostructures via DC Reactive Magnetron Sputtering Technique", *Iraqi J. Appl. Phys.*, 19(4C) (2023) 229-234.

[47] Z. Gonzalez et al., "Electrophoretic deposition of binder-free TiN nanoparticles to design 3D microstructures. The role of sintering in the microstructural robustness of supercapacitor electrodes", *Electrochimica Acta*, 369 (2021) 137654.

[48] A.M. Hassan, P.M. Millner and J.G. McAlley, "Characterization of Indium Nitride Thin Films Prepared by Plasma-Assisted Molecular Beam Epitaxy", *Iraqi J. Appl. Phys.*, 18(3) (2022) 19-24.

[49] Y. Xie et al., "TiN nanoparticles anchored on porous carbon black: The synergistic effect of porosity, surface roughness and surface plasmon on high-performance broadband infrared absorption", *Infrared Phys. Technol.*, 147 (2025) 105819.

[50] M. Abbasi-Nahr, S.E. Mirsalehi and S.S. Mirhosseini, "Additive manufacturing of AA5083/TiN-Diamond hybrid nanocomposite parts via additive friction stir deposition: Metallurgical structure, mechanical, tribological, and electrochemical properties", *J. Mater. Res. Technol.*, 30 (2024) 8187-8208.

[51] M. Chisaka et al., "Synthesis of carbon-supported titanium oxynitride nanoparticles as cathode catalyst for polymer electrolyte fuel cells", *Electrochimica Acta*, 113 (2013) 735-740.

[52] N. Vidakis et al., "On the thermal and mechanical performance of Polycarbonate/Titanium Nitride nanocomposites in material extrusion additive manufacturing", *Composites C: Open Access*, 8 (2022) 100291.

[53] O.E. Falodun et al., "Spark Plasma Consolidation and Wear Behaviour of Nanoceramic addition into Titanium Alloy", *Mater. Today: Proc.*, 18(7) (2019) 2234-2241.

[54] Z.H. Zaidan, Q.H. Mahmood and O.A. Hammadi, "Using Banana Peels for Green Synthesis of Mixed-Phase Titanium Dioxide Nanopowders", *Iraqi J. Appl. Phys.*, 18(4) (2022) 27-30.

[55] Z.H. Zaidan, O.A. Hammadi and K.H. Mahmood, "Effect of Structural Phase on Photocatalytic Activity of Titanium Dioxide Nanoparticles", *Iraqi J. Appl. Phys.*, 19(3A) (2023) 55-58.

[56] E.A. Al-Oubidy and F.J. Al-Maliki, "Effect of Gas Mixing Ratio on Energy Band Gap of Mixed-Phase Titanium Dioxide Nanostructures Prepared by Reactive Magnetron Sputtering Technique", *Iraqi J. Appl. Phys.*, 14(4) (2018) 19-23.

[57] F.J. Al-Maliki and E.A. Al-Oubidy, "Effect of gas mixing ratio on structural characteristics of titanium dioxide nanostructures synthesized by DC reactive magnetron sputtering", *Physica B: Cond. Matter*, 555 (2019) 18-20.

[58] F.J. Al-Maliki, O.A. Hammadi and E.A. Al-Oubidy, "Optimization of Rutile/Anatase Ratio in Titanium Dioxide Nanostructures prepared by DC Magnetron Sputtering Technique", *Iraqi J. Sci.*, 60(special issue) (2019) 91-98.

[59] E.A. Al-Oubidy and F.J. Al-Maliki, "Photocatalytic activity of anatase titanium dioxide nanostructures prepared by reactive magnetron sputtering technique", *Opt. Quantum Electron.*, 51(1-2) (2019) 23.

[60] O.A. Hammadi, F.J. Kadhim and E.A. Al-Oubidy, "Photocatalytic Activity of Nitrogen-Doped Titanium Dioxide Nanostructures Synthesized by DC Reactive Magnetron Sputtering Technique", *Nonl. Opt. Quantum Opt.*, 51(1-2) (2019) 67-78.

[61] R.A.H. Hassan and F.T. Ibrahim, "Preparation and Characterization of Anatase Titanium Dioxide Nanostructures as Smart and Self-Cleaned Surfaces", *Iraqi J. Appl. Phys.*, 16(4) (2020) 13-18.

[62] O.A. Hammadi, "Production of Nanopowders from Physical Vapor Deposited Films on Nonmetallic Substrates by Conjunctional Freezing-Assisted Ultrasonic Extraction Method", *Proc. IMechE, Part N, J. Nanomater. Nanoeng. Nanosys.*, 232(4) (2018) 135-140.

[63] O.A. Hammadi, "Effects of Extraction Parameters on Particle Size of Titanium Dioxide Nanopowders Prepared by Physical Vapor Deposition Technique", *Plasmonics*, 15(6) (2020) 1747-1754.

 © ALL RIGHTS RESERVED